

# Supporting Information

## Surface-induced 2D/1D Hetero-structured Growth of ReS<sub>2</sub>/CoS<sub>2</sub> for High Performance Electro-catalyst

*Yuanwu Liu<sup>1</sup>, Jing Li<sup>1</sup>, Wentian Huang<sup>1</sup>, Ying Zhang<sup>1</sup>, Minjie Wang<sup>1</sup>, Xingsen Gao<sup>1</sup>, Xin Wang<sup>2</sup>, Mingliang Jin<sup>2</sup>, Zhipeng Hou<sup>1\*</sup>, Guofu Zhou<sup>2</sup>, Zhang Zhang<sup>1,2\*</sup>, Junming Liu<sup>1,3</sup>*

1. Guangdong Provincial Key Laboratory of Quantum Engineering and Quantum Materials, Institute for Advanced Materials, South China Academy of Advanced Optoelectronics, South China Normal University, Guangzhou 510006, P. R. China
2. National Center for International Research on Green Optoelectronics, South China Academy of Advanced Optoelectronics, South China Normal University, Guangzhou 510006, P. R. China
3. Laboratory of Solid State Microstructure, Nanjing University, Nanjing 210093, P. R. China

### Corresponding Author

\*E-mail: [zzhang@scnu.edu.cn](mailto:zzhang@scnu.edu.cn) (Zhang Zhang)

\*E-mail: [houzp@m.scnu.edu.cn](mailto:houzp@m.scnu.edu.cn) (Zhipeng Hou)

### Calculation of lattice mismatch of ReS<sub>2</sub>/CoS<sub>2</sub>

The cell parameters of CoS<sub>2</sub> and ReS<sub>2</sub> are shown below: CoS<sub>2</sub> (JCPDS 41-1471; space group *Pa3*;  $a = 5.5376 \text{ \AA}$ ), ReS<sub>2</sub> (JCPDS 52-0818; space group *PI*;  $a = 6.45 \text{ \AA}$ ).

According to the calculation formula of lattice mismatch degree of semiconductor heterojunction<sup>1</sup>, the mismatch degree is 15.22%.

$$\delta = \frac{2|a_{\text{CoS}_2} - a_{\text{ReS}_2}|}{a_{\text{CoS}_2} + a_{\text{ReS}_2}} = 15.22\%$$

### Supplementary figures

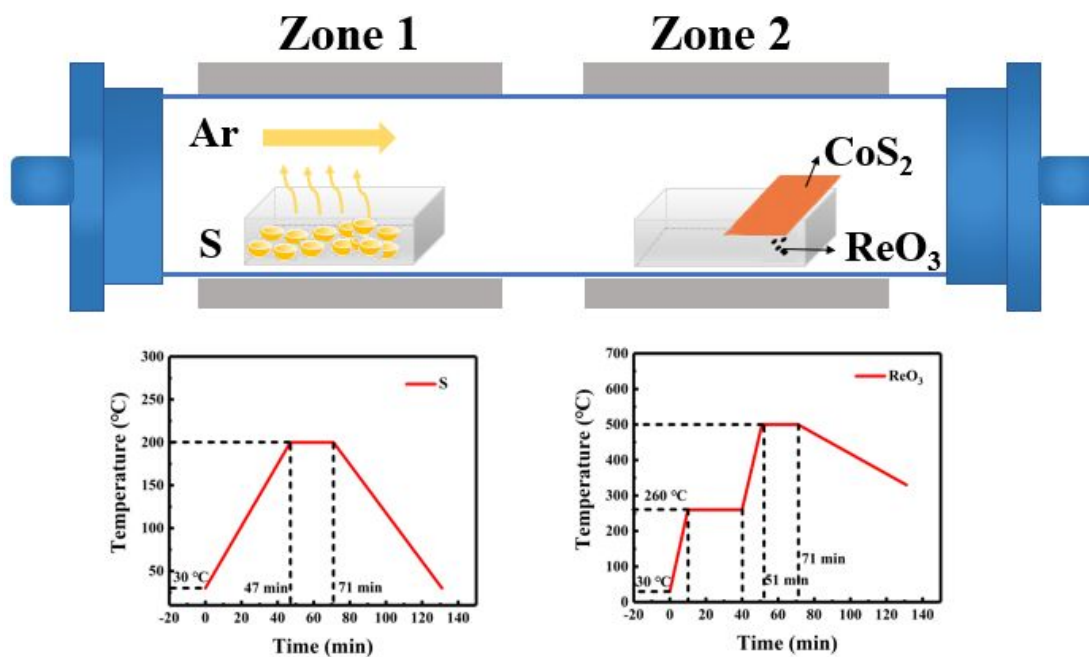


**Figure S1.** Schematic of the controlled synthesis of ReS<sub>2</sub> via CVD method.

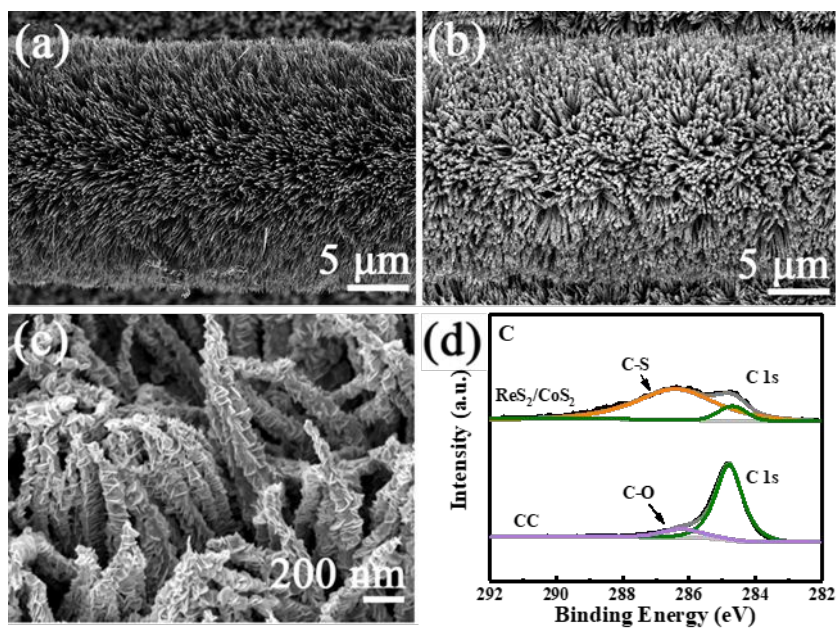


**Figure S2.** (a) Low-magnification SEM image of large scale  $\text{CoS}_2$  nanowire arrays. (b) Low-magnification SEM image of  $\text{ReS}_2/\text{CoS}_2$ . (c) High-magnification SEM image of high density  $\text{ReS}_2$  nanosheets distributed on  $\text{CoS}_2$  nanowires. (d) High-resolution XPS spectrum of C 1s in  $\text{ReS}_2/\text{CoS}_2$  and bare carbon cloth.

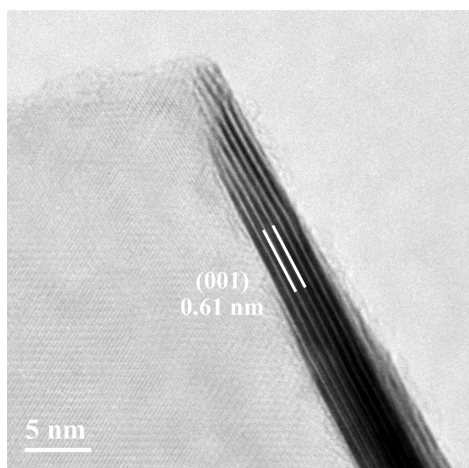


**Figure S3.** TEM image of a  $\text{ReS}_2$  nanosheet.

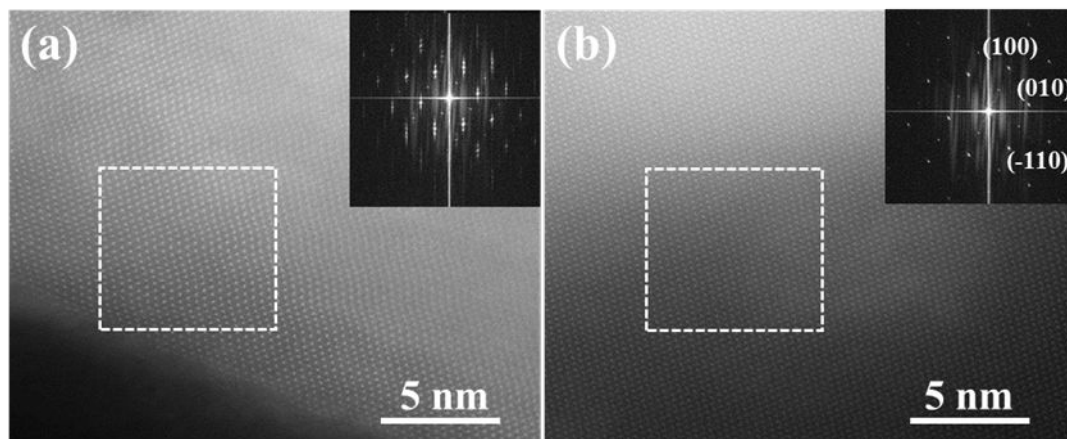


**Figure S4.** (a) STEM image of ReS<sub>2</sub> at the interface of ReS<sub>2</sub>/CoS<sub>2</sub>. (b) STEM image of ReS<sub>2</sub> away from the interface ReS<sub>2</sub>/CoS<sub>2</sub>. Inset in Figure a and b are corresponding FFT images.

#### **S5. Morphology and structure characterization of ReS<sub>2</sub>/CoP**

As shown in Figure S5a, the crystal structures were investigated by X-ray diffraction (XRD). The characteristic peaks at 14.4°, 15.9°, 16.1°, 16.7°, 20.4°, 21.9° and 28.5° were ascribed to the (002), (010), (-110), (100), (-112), (003) and (110) of ReS<sub>2</sub> (PDF No. 89-0341). Other peaks were consistent with standard CoP, confirming that the composite was ReS<sub>2</sub>/CoP<sup>2</sup>. High density 1D CoS<sub>2</sub> nanowires were uniformly distributed on the pure CC (Figure S3b). As displayed in Figure S3c, irregular ReS<sub>2</sub> nanosheets with a diameter of 200 nm are observed. However, the density of ReS<sub>2</sub> wasn't large and it was nearly grown at the tip of CoP nanowire. In Figure S3d, the element mapping of ReS<sub>2</sub>/CoP manifested that the intimate contact between ReS<sub>2</sub> and CoP in ReS<sub>2</sub>/CoP with uniform distribution of the S element. But S content wasn't high, indicating that S could only be replaced with a part of phosphorus in the same

time. All of these confirm that  $\text{ReS}_2/\text{CoP}$  was successfully synthesized.

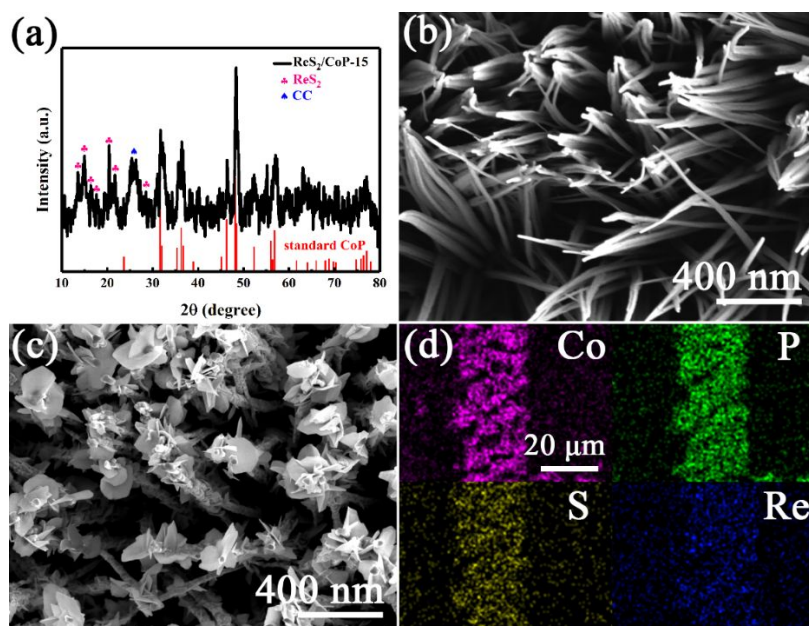


**Figure S5.** (a) XRD pattern of  $\text{ReS}_2/\text{CoP}$ . (b) SEM image of high-density CoP nanowires. (c) Low-magnification SEM image of  $\text{ReS}_2/\text{CoP}$ . (d) EDX elemental mapping images of Co, P, S and Re element distribution.

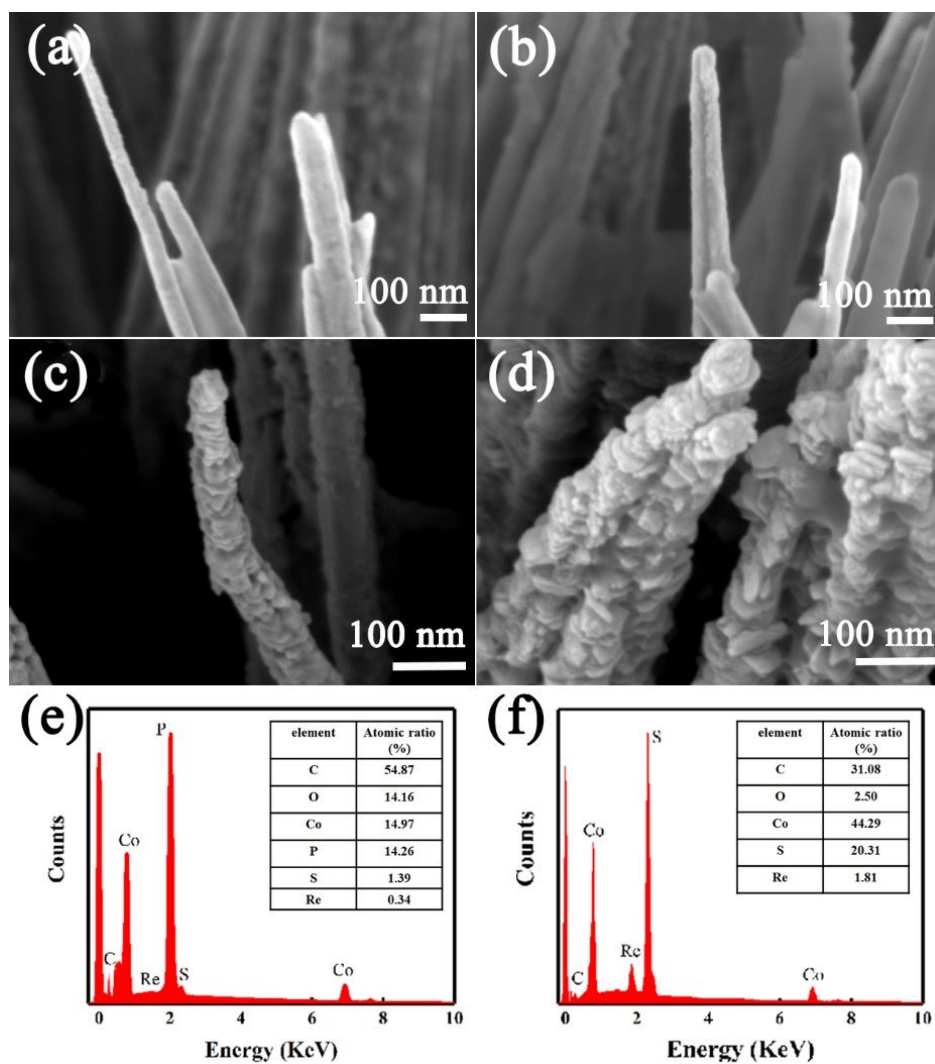


**Figure S6.** High-magnification SEM image of (a) CoP nanowires, (b) ReS<sub>2</sub>/CoP-5, (c) CoS<sub>2</sub> nanowires and (d) ReS<sub>2</sub>/CoS<sub>2</sub>-5. (e, f) EDX spectra of ReS<sub>2</sub>/CoP-5 and ReS<sub>2</sub>/CoS<sub>2</sub>-5, respectively. Insets in e and f are the atomic ratio of each element.

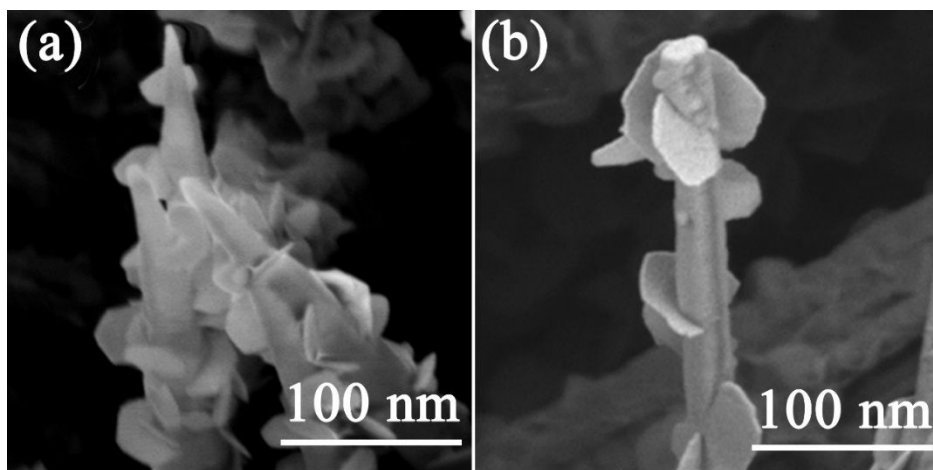


**Figure S7.** High-magnification SEM images of (a) ReS<sub>2</sub>/CoS<sub>2</sub>-10 and (b) ReS<sub>2</sub>/CoP-10.

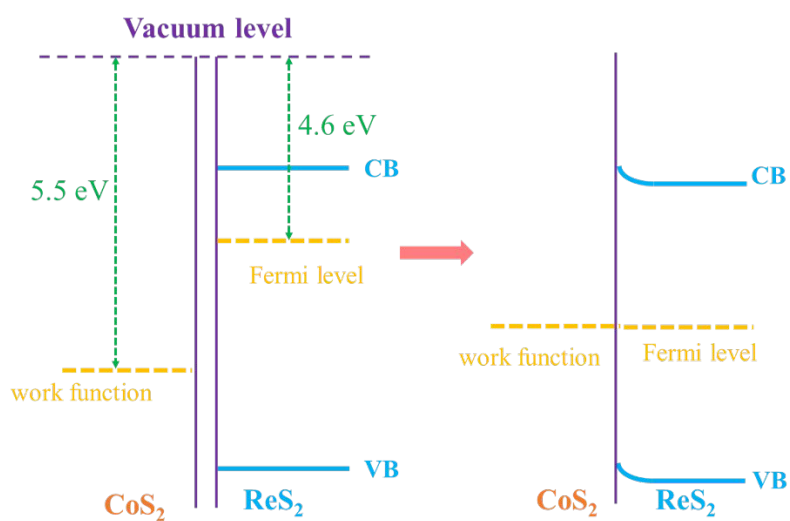


**Figure S8.** Band alignment diagram between CoS<sub>2</sub> and ReS<sub>2</sub>.



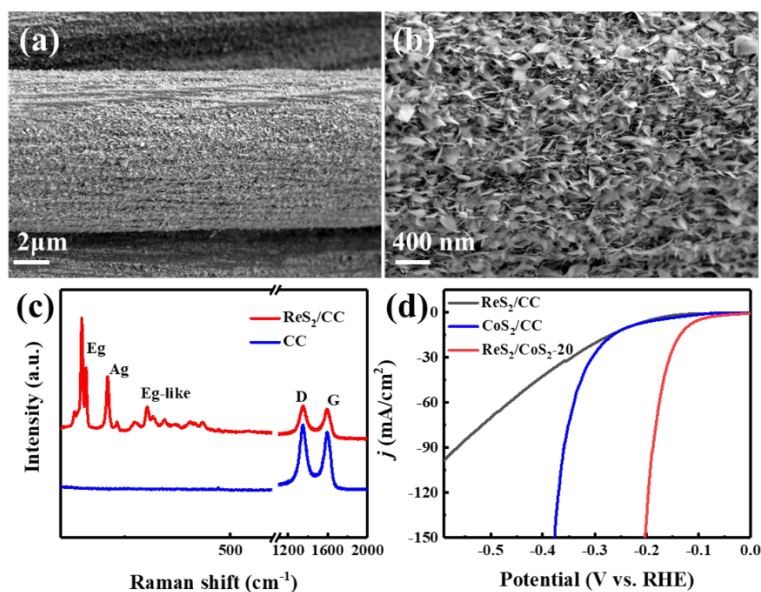


**Figure S9.** (a, b) SEM images of ReS<sub>2</sub>/CC. (c) Raman spectrum of ReS<sub>2</sub>/CC and CC. (d) HER polarization curves of ReS<sub>2</sub>/CC, CoS<sub>2</sub>/CC and ReS<sub>2</sub>/CoS<sub>2</sub>-20.

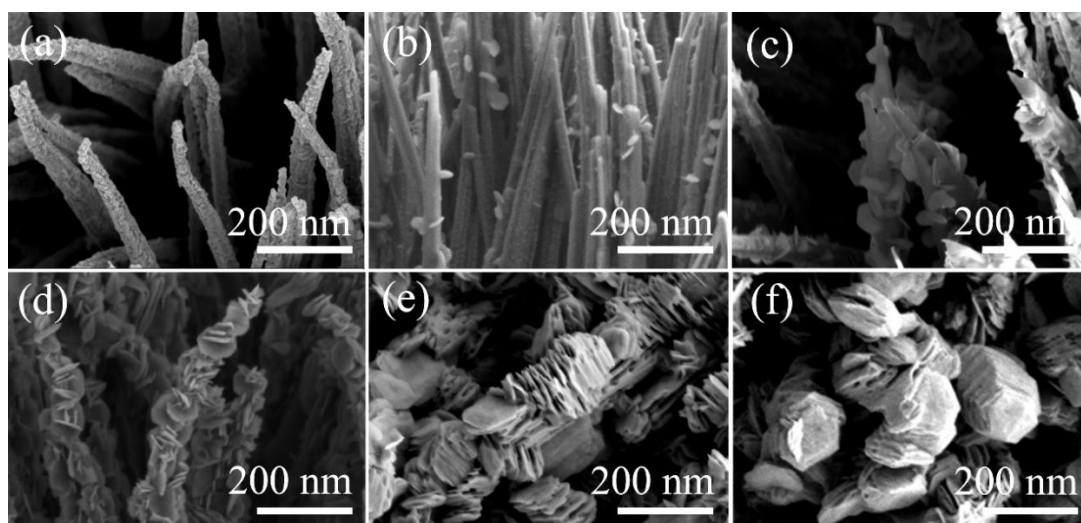


**Figure S10.** SEM image of ReS<sub>2</sub> with different growth time (a) 0 min, (b) 10 min, (c) 15 min, (d) 20 min and (e) 25 min on CoS<sub>2</sub> nanowires. (f) high-magnification SEM image in c.



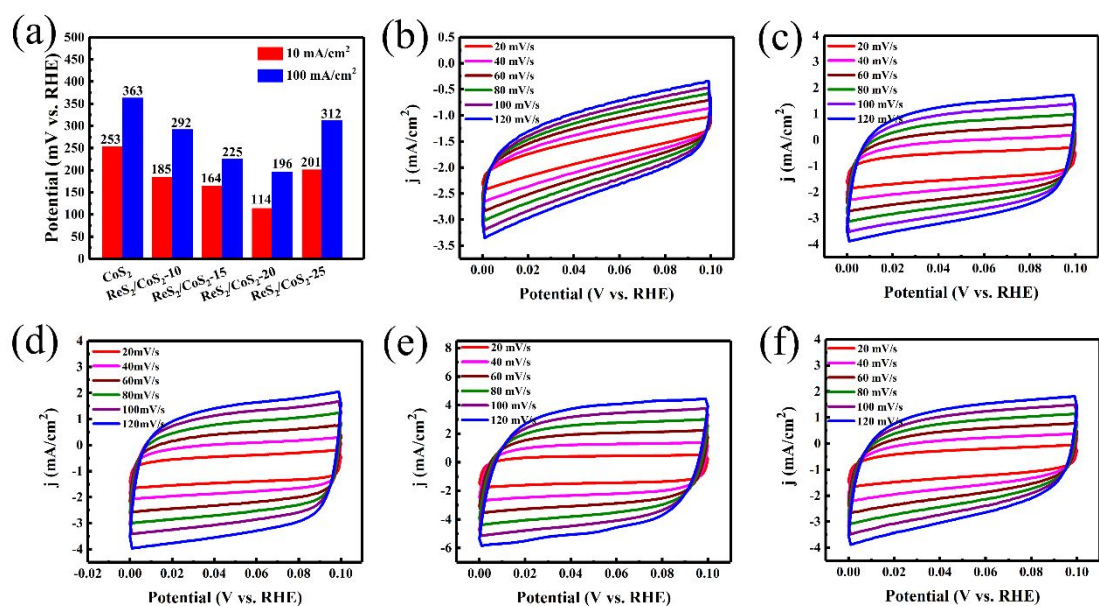


**Figure S11.** (a) The overpotential of CoS<sub>2</sub>, ReS<sub>2</sub>/CoS<sub>2</sub>-10, ReS<sub>2</sub>/CoS<sub>2</sub>-15, ReS<sub>2</sub>/CoS<sub>2</sub>-20 and ReS<sub>2</sub>/CoS<sub>2</sub>-25 at 10 mA/cm<sup>2</sup> and 100 mA/cm<sup>2</sup>, respectively. (b) CoS<sub>2</sub>, (c) ReS<sub>2</sub>/CoS<sub>2</sub>-10, (d) ReS<sub>2</sub>/CoS<sub>2</sub>-15, (e) ReS<sub>2</sub>/CoS<sub>2</sub>-20 and (f) ReS<sub>2</sub>/CoS<sub>2</sub>-25 are the CV curves at different scan rates.

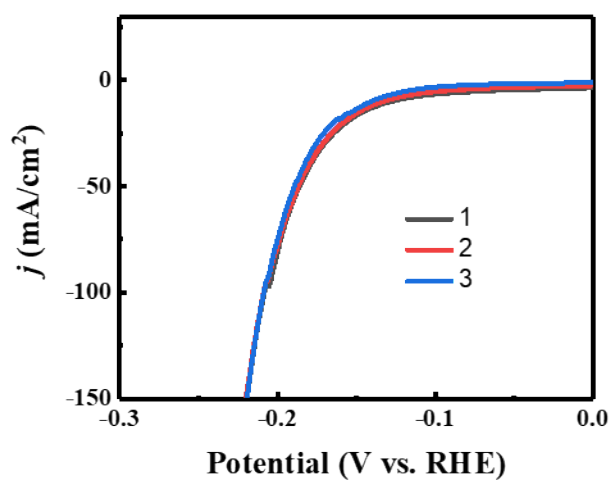


**Figure S12.** HER polarization curves of different batches of ReS<sub>2</sub>/CoS<sub>2</sub>-20.

**Table S1.** Electrochemical performances of Pt/C.

samples	$\eta$ (mV vs RHE) for $j=10$ $\text{mA}/\text{cm}^2$	Tafel slope (mV/dec)	Refs
Pt/C	50	34	3
Pt/C	48	44	10
Pt/C	62	33	8
Pt/C	33	30	11
Pt/C	78	42	12
Pt/C	49	42	13
Pt/C	28	43	This work

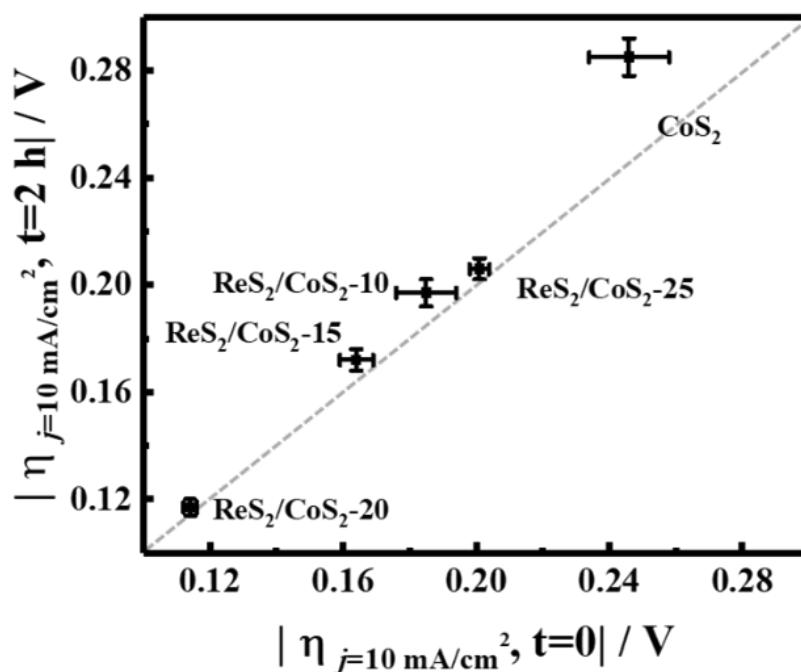


**Figure S13.** Plots of catalytic activity, stability, and electrochemically-active surface area for HER electrocatalysts in acidic solutions. The x-axis is the overpotential required to achieve 10 mA cm<sup>-2</sup> per geometric area at time t = 0. The y-axis is the overpotential required to achieve 10 mA cm<sup>-2</sup> per geometric area at time t = 2 h. The diagonal dashed line is the expected response for a stable catalyst that does not change in activity during 2 h constant polarization.

**Table S2. Electrochemical performances of CoS<sub>2</sub>-based and ReS<sub>2</sub>-based catalysts.**

samples	$\eta$ (mV vs RHE) for $j=10$ $\text{mA}/\text{cm}^2$	Tafel slope (mV/dec)	Refs
$\text{CoS}_{2x}\text{Se}_{2(1-x)}$ nanowire array	129.5	68.7	3
$\text{CoS}_2\text{-C@MoS}_2$	173	67	4
$\text{MoO}_2/\text{MoS}_2/\text{CoS}_2$	123	133	5
$\text{V}_{\text{Re}}\text{-ReS}_2$	147	69	6
Sunflower-shaped $\text{ReS}_2$	270	76	7
$\text{NiS}_2/\text{CoS}_2/\text{C}$	165	72	8
Li-vertical $\text{ReS}_2\text{@Au}$	201	84	9
$\text{ReS}_2/\text{CoS}_2$	114	63.7	This work

## References

- (1) Jacques, A.; Diologent, F.; Bastie, P. In Situ Measurement of the Lattice Parameter Mismatch of a Nickel-Base Single-Crystalline Superalloy under Variable Stress. *Mater. Sci. Eng. A* **2004**, *1*, 387–389.
- (2) Tian, J.; Chen, J.; Liu, J.; Tian, Q.; Chen, P. Graphene Quantum Dot Engineered Nickel-Cobalt Phosphide as Highly Efficient Bifunctional Catalyst for Overall Water Splitting. *Nano Energy* **2018**, *48*, 284–291.
- (3) Liu, K.; Wang, F.; Xu, K.; Shifa, T. A.; Cheng, Z.; Zhan, X.; He, J.  $\text{CoS}_{2x}\text{Se}_{2(1-x)}$  Nanowire Array: An Efficient Ternary Electrocatalyst for the Hydrogen Evolution Reaction. *Nanoscale* **2016**, *8*, 4699–4704.
- (4) Zhu, Y.; Song, L.; Song, N.; Li, M.; Wang, C.; Lu, X. Bifunctional and Efficient  $\text{CoS}_2\text{-C@MoS}_2$  Core-Shell Nanofiber Electrocatalyst for Water Splitting. *ACS Sustain. Chem. Eng.* **2019**, *7*, 2899–2905.
- (5) Wang, Y.; Zhu, Y.; Afshar, S.; Woo, M. W.; Tang, J.; Williams, T.; Kong, B.;

- Zhao, D.; Wang, H.; Selomulya, C. One-Dimensional CoS<sub>2</sub>-MoS<sub>2</sub> Nano-Flakes Decorated MoO<sub>2</sub> Sub-Micro-Wires for Synergistically Enhanced Hydrogen Evolution. *Nanoscale* **2019**, *11*, 3500–3505.
- (6) Zhou, Y.; Song, E.; Zhou, J.; Lin, J.; Ma, R.; Wang, Y.; Qiu, W.; Shen, R.; Suenaga, K.; Liu, Q. Auto-Optimizing Hydrogen Evolution Catalytic Activity of ReS<sub>2</sub> through Intrinsic Charge Engineering. *ACS Nano* **2018**, *12*, 4486–4493.
- (7) Huang, J.; Gao, H.; Xia, Y.; Sun, Y.; Xiong, J.; Li, Y.; Cong, S.; Guo, J.; Du, S.; Zou, G. Enhanced Photoelectrochemical Performance of Defect-Rich ReS<sub>2</sub> Nanosheets in Visible-Light Assisted Hydrogen Generation. *Nano Energy* **2018**, *46*, 305–313.
- (8) Xin, W.; Jiang, W. J.; Lian, Y.; Li, H.; Hong, S.; Xu, S.; Yan, H.; Hu, J. S. NiS<sub>2</sub> Nano dotted Carnation-like CoS<sub>2</sub> for Enhanced Electrocatalytic Water Splitting. *Chem. Commun.* **2019**, *55*, 3781–3784.
- (9) Gao, J.; Li, L.; Tan, J.; Sun, H.; Li, B.; Idrobo, J. C.; Singh, C. V.; Lu, T.-M.; Koratkar, N. Vertically Oriented Arrays of ReS<sub>2</sub> Nanosheets for Electrochemical Energy Storage and Electrocatalysis. *Nano Lett.* **2016**, *16*, 3780–3787.
- (10) Zhang, H.; Li, Y.; Xu, T.; Wang, J.; Huo, Z.; Wan, P.; Sun, X. Amorphous Co-Doped MoS<sub>2</sub> Nanosheet Coated Metallic CoS<sub>2</sub> Nano cubes as an Excellent Electrocatalyst for Hydrogen Evolution. *J. Mater. Chem. A* **2015**, *3*, 15020–

15023.

- (11) Zhang, J.; Liu, Y.; Sun, C.; Xi, P.; Peng, S.; Gao, D.; Xue, D. Accelerated Hydrogen Evolution Reaction in CoS<sub>2</sub> by Transition-Metal Doping. *ACS Energy Lett.* **2018**, *3*, 779–786.
- (12) Zhang, Q.; Ye, C.; Li, X. L.; Deng, Y. H.; Tao, B. X.; Xiao, W.; Li, L. J.; Li, N. B.; Luo, H. Q. Self-Interconnected Porous Networks of NiCo Disulfide as Efficient Bifunctional Electrocatalysts for Overall Water Splitting. *ACS Appl. Mater. Interfaces* **2018**, *10*, 27723–27733.
- (13) Wen, L.; Sun, Y.; Zhang, C.; Yu, J.; Li, X.; Lyu, X. Cu-Doped CoP Nanorod Arrays : Efficient and Durable Hydrogen Evolution Reaction Electrocatalysts at All PH Values. *ACS Appl. Energy Mater.* **2018**, *1*, 3835-3842.